International Journal of Engineering Research & Technology (IJERT)
ISSN: 2278-0181
Vol. 1 Issue 8, October - 2012

Structural And Magnetic Properties Of Mg Substituted Ni- Co Nanocrystalline Ferrite By Auto-Combustion Technique

S.M.Rathod [*] **, *S.V. Gaikwad, S.S.Jagtap,***

P.G &Research Department of Physics, Abasaheb Garware College, Karve Road, Pune-411004, Maharashtra, INDIA

Abstract

Sol-gel auto combustion is a unique combination of the combustion and the chemical gelation processes. Structural and magnetic properties of Mg^{2+} substituted $Mg_xNi_{0.8-x}Co_{0.2}Fe_2O_4$ ferrites for x = 0.2, 0.4, 0.6 prepared by an auto-combustion method have been investigated. The nano size powders with compositions $MgNiCoFe_2O_4$ were synthesized by sol-gel combustion method. The puffy, porous brown powder – as combusted was calcined at temperature of 400^0C for 4 hour. Saturation magnetization decreased from 40 emu/g to 32 emu/g for sintered at400^o C . These nanoferrites may have application in core materials and in electronic device technology. The prepared materials were confirmation of ferrite bonds studied by IR spectroscopy. The X-ray diffraction pattern of these compositions confirmed the formation of the nanocrystalline structure. Further, the XRD have been used to calculate the lattice parameter and grain size. The particle size of the synthesized compositions materials are varying from 23 nm to 21 nm. Transmission electron microscopy (TEM) and Scanning electron microscopy (SEM) respectively. The morphological investigations and nanometric sizes of the samples was studied by using scanning electron microscopy and transmission electron microscopic techniques. The average particle size was estimated about 20-25 nm for calcined powders .UV visible spectroscopy of the material taken by UV-source" Perkin Eimer Lembda-25" it found to be the prepared material in the range of semiconductor in nature. Transmission electron microscopy (TEM) SADE found to be material is crystalline in nature.

Keywords: *Sol-gel auto-combustion, Nanocrystalline, $MgNiCoFe_2O_4$, IR-Spectroscopy, X-ray diffraction, Scanning electron microscopy, Vibrating Sample microscopy, UV-Visible Spectroscopy, Transmission electron microscopy (TEM).*

Corresponding Author: Dr. Rathod S. M., P. G. And Research Department of Physics, Abasaheb Garware College, Karve Road, Pune-311003, [INDIA]

1. Introduction

The sol-gel auto-ignition method is used to speed up the synthesis of complex materials. It is the simple process, a significant saving in time and energy consumption over the traditional methods. This method is employed to obtain improved power characteristics, more homogeneity and have a narrow particle size, thereby influencing structural, electrical and magnetic properties of spinel ferrites [1]. Promising future applications of ferrite nanoparticles in medicine, making many devices like permanent magnets, memory storage devices etc. Ferrite nanoparticles have been the emerging focus of the recent scientific research.

Spinel ferrites are an important class of compounds having large variety of electronic, magnetic and catalytic properties as they possess high resistivity and negligible eddy current losses. Ferrites are magnetic ceramics of great importance in the production of electronic components. Their

applications range from simple function devices, such as small permanent magnets, to sophisticated devices for the electro-electronic industry. Some interesting applications of these materials are in computer peripherals, telecommunication equipment, permanent magnets, electronic, and magnetic media used in computers, recording devices and magnetic cards. The electrical and magnetic properties are the most important properties for ferrites depending on the processing conditions, sintering temperature, sintering time, chemical composition and the amount and type of the additives [2].The sol-gel chemical methods have given numerous advantages in terms of the properties and simplicity of the technique. The investigations on the nano-crystalline ferrite particles containing nickel and zinc using the sol-gel methods have been given much attention. However, the principle requirements of the ferrites have been less reported. The sol-gel route is relatively a new technique that uses organic compounds to produce ferrite cores, which at the moment imposes a high cost in its chosen starting materials [3-4].

The magnetic properties of the nanosized ferrites are entirely different from those of their bulk counterparts, such as the super-paramagnetic behaviour and associated properties. Nanosized ferrites with uniform particle size and narrow size distribution are desirable for a variety of applications like targeted drug delivery, ferrofluids, medical imaging and other biomedical applications, magnetic data storage, etc., [5-8].ll manuscripts must be in English. These guidelines include complete descriptions of the fonts, spacing, and related information for producing your proceedings manuscripts. Ferrite nanocrystals are also of interest in various applications, such as inter-body drug delivery [9-11], bioseparation, and magnetic refrigeration systems [12-16], as they exhibit superparamagnetism

2. Experimental

2.1. Synthesis of nanoferrite:

Mg substituted Ni-Co nanocrystalline ferrite $Mg_xNi_{0.8-x}Co_{0.2}Fe_2O_4$ (where x = 0.2, 0.4, 0.6) were prepared by sol-gel auto-combustion technique. The precursor solution was prepared using AR grade metal nitrates; $Mg(NO_3)_2$, $Co(NO_3)_2$, $Ni(NO_3)_2$, and $Fe_2(NO_3)_2$. These nitrates were initially dissolved separately in distilled water and stirred well for 20 minutes at 80° C, subsequently the precursor solution was prepared by adding all above solutions and continuously stirred for 30 minutes at 80° C. An aqueous solution of citric acid mixed with metal nitrate solution, and then ammonia solution was slowly added to adjust the pH at 7. The mixed solution was kept on to a hot plate with continuous stirring at 100° C. When finally all water molecules were removed from the mixture, the viscous gel began frothing.

The materials used in this procedure for the preparation of MgNiCo ferrite are analytical grade of Magnesium nitrate, Nickel nitrate, Cobalt nitrate, Iron nitrate, and citric acid. The materials are weighed according to the required stoichiometric ratio. These nitrates and citrate were dissolved in suitable amount deionised water which was magnetically stirred at 75°C until the mixture was homogenized. Liquid ammonia was added to the solution to adjust the pH value about 7. During this procedure the solution was continuously stirred using a magnetic stirrer. Then the mixed solution was heated at 100°C with constant stirring to transform it into a xerogel. When ignited at any point, the dried gel burnt in a self-propagating combustion manner until all the gel was burnt out completely to form a loose powder.

3. Results and Discussions:

A. Infra Red Characterization

The disappearance of the characteristic bands of carboxyl group and $(NO)_3$ ion in the IR spectrum curve after combustion revealed that the carboxyl group and the $(NO)_3$ ion take part in the reaction during combustion. Therefore, the combustion can be considered as a thermally induced anionic redox reaction of the gel where in the citrate ion acts as a reductant and the nitrate ion acts as an oxidant. Because the nitrate ions provide an in situ oxidizing environment for the decomposition of the organic component, the rate of the oxidation reaction relatively increases.

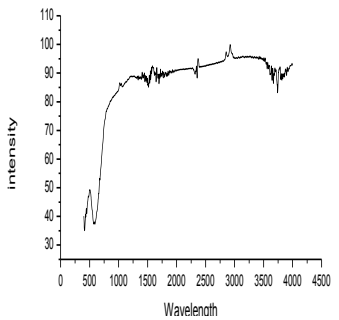

FIGURE 1: IR graph of $MgNiCoFe_2O_4$

B. X-Ray Diffraction

The phase formation behavior of $Mg_xNi_{0.8-x}Co_{0.2}Fe_2O_4$ (where x = 0.2, 0.4, 0.6) was studied by XRD There was no metal oxide phase in the as burnt powder. The crystallite size was calculated from Full Width at Half Maximum (FWHM) for all the peaks using Scherrer formula:

$$t = \frac{0.9\lambda}{\beta \cos\theta} \qquad (1)$$

β=full width at half maximum, θ=bragg angle for the actual peak.

The lattice parameter was calculated by using the following formula:

$$sin^2\theta = \frac{\lambda^2}{4a^2}(h^2 + k^2 + l^2) \qquad (2)$$

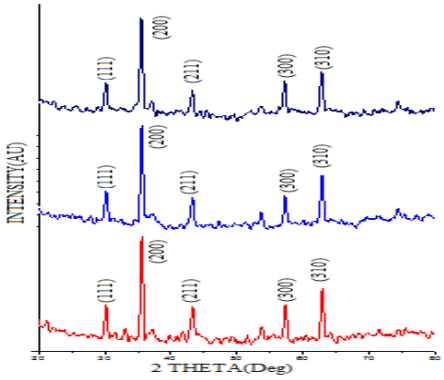

FIGURE 2: XRD graph of MgNiCo ferrite where x The size of the particle is observed to be increased with increase in sintering temperature. While sintering generally decreases the lattice defects and strains, however it can also cause coalescence of crystallites that result in increasing the average size of the nanoparticles [17]

C. Vibrating Sample Microscopy

Saturation Magnetization has been determined from the force experienced by the ferrite specimen in the field gradient. It was measured using Vibrating Sample Magnetometer (VSM) (model 7307, Lake Shore). The principle of VSM is the measurement of electromotive force induced by magnetic sample when it is vibrated at constant frequency in the presence of a static and uniform magnetic field. A small part of sintered powder (0.0125 g) was weighted and made to avoid movements inside the sample holder. The VSM was operated to 1 Tesla. Fig. 4 shows the magnetization curve of the $MgNiCoFe_2O_4$. as increasing the percentage of Mg the magnetization, coercivity and retentivity decrease.

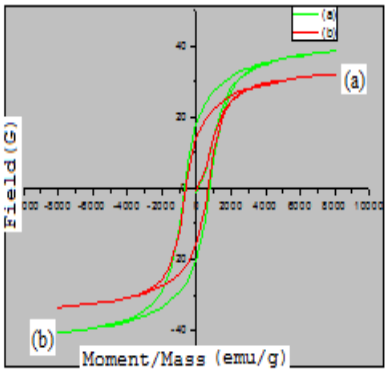

FIGURE 3 :VSM of $MgNiCoFe_2O_4$ (a)$Mg_{0.2}Ni_{0.6}Co_{0.2}Fe_2O_4$

(b) $Mg_{0.6}Ni_{0.2}Co_{0.2}Fe_2O_4$

D. Scanning Electron Microscopy

The structural morphology for different proportions of $Mg_xNi_{0.8-x}Co_{0.2}Fe_2O_4$ (where x = 0.2, 0.4, 0.6) is studied by using scanning electron microscopy. The Figure 3 shows SEM graphs of the MgNiCo ferrite revealed that this material doesn't have a specific morphology and average grain sizes of the samples are determined from these micrographs..

. This result agrees with the result for Zn^{2+}, Cd^{2+}, Ti^{4+} substituted ferrites [17, 18]. At low composition, formation of large exaggerated grains of non-uniform size is seen to occur. The driving force for grain growth is the surface tension of the grain boundary [19].

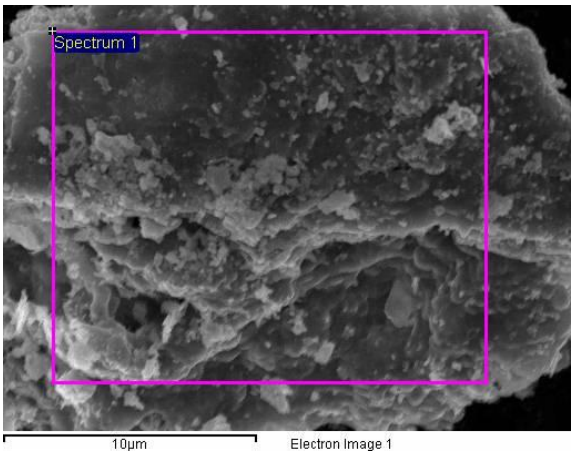

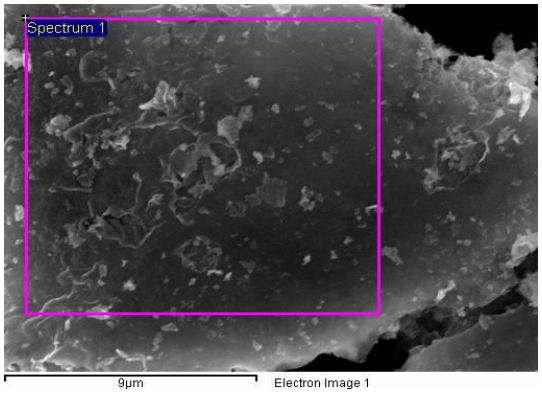

FIGURE4:SEM,

$Mg_xNi_{x0.6}Co_{0.2}Fe_2O_4$.wherex=0.2,0.4,0.6

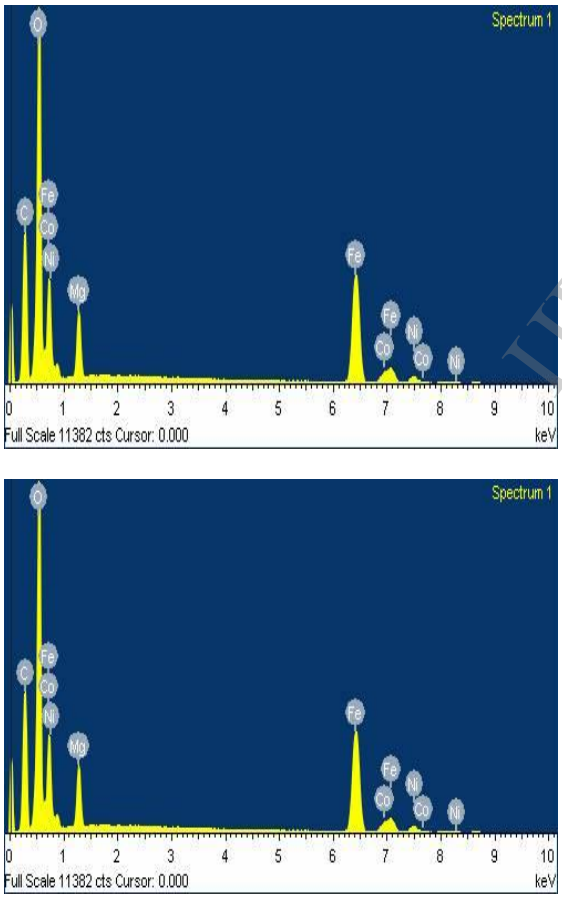

FIGURE5:SEM,
$Mg_xNi_{x0.6}Co_{0.2}Fe_2O_4$.wherex=0.2,0.6

E. UV-Spectroscpoy

The figure (5) shows the UV-Visible spectroscopy absorption and reflection in the UV region. In the absorption molecules of Π-electron or non –bonding (n-electron) can absorb the energy in the form of ultraviolet or visible light to excite this electron to higher or anti-bonding molecular orbit [20]. The band gap energy was calculated by following formula. The results of the samples have great influence on their optical property [21].

$$E = \frac{hc}{\lambda}$$

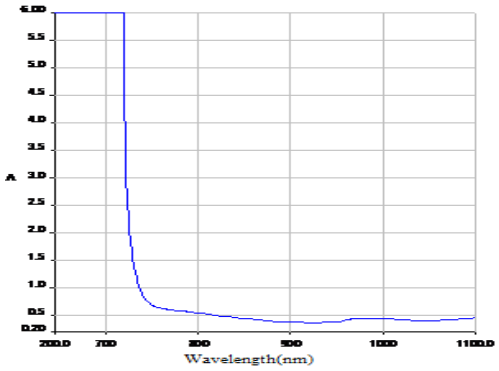

FIGURE6:UV-Specrta.

F.Transmission Electron Microscopy

The TEM micrograph of the synthesized nano particles along with selected electron diffraction (SAED) for $Mg_xNi0_{8-x}Co_{0.2}Fe_2O_4$ ferrite shown in fig.2 a,b., fig.3 a,b. fig 4 a,b .The TEM micrographs shows the particles have a size distribution 20 to 25 nm (±1nm) .The agglomeration formed because they experience a permanent magnetic moment proportional to their volume[11].The SAED image of synthesized nano particles ,distinct ring that conforms good crystallinity are clearly visible.

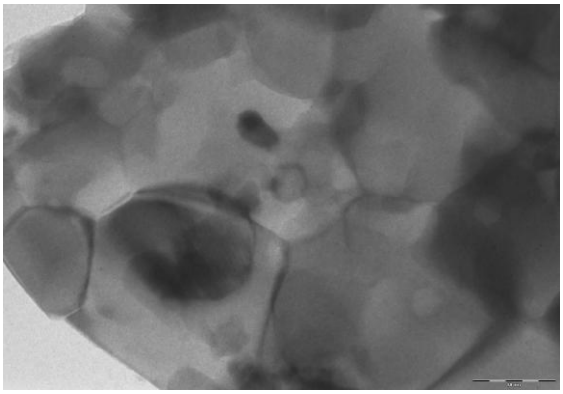

(a)

It has been observed that particles are aggregated during annealing and metal ion incorporation. The

crystalline lattice fringe is observed as uniformly extended over the primary building blocks, grain boundaries and pores in the samples annealed at 400^{o} C for all compositions. Thus it can be concluded that the nanoparticles are organized in to an isooriented attached structure by sharing identical lattice planes.

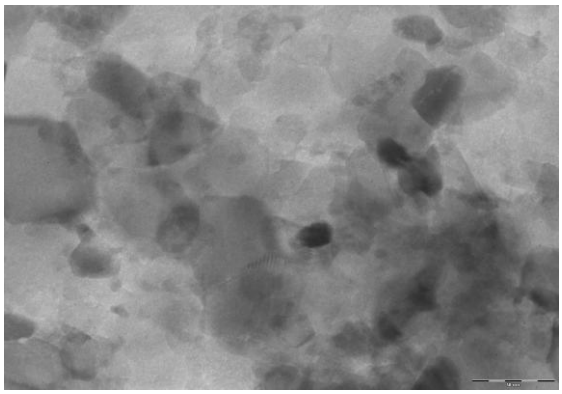

(b)

FIGURE7:TEM $Mg_xNi_{x-0.6}Co_{0.2}Fe_2O_4$.(a)0.2(b)0.6.

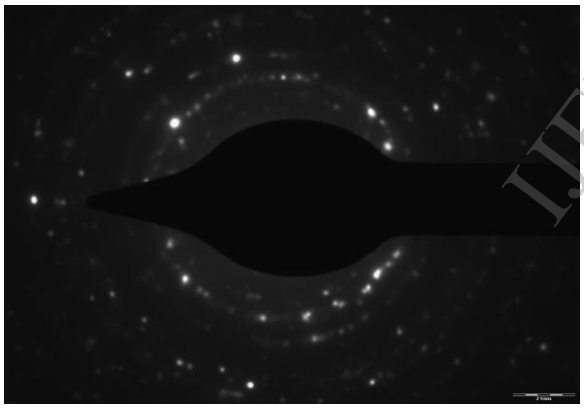

(a)

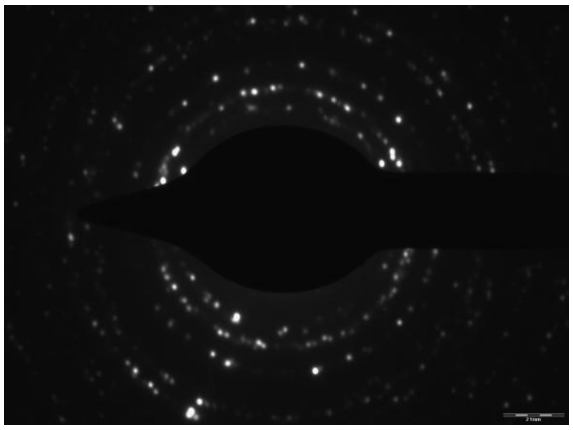

(b)

FIGURE8:TEM $Mg_xNi_{x-0.6}Co_{0.2}Fe_2O_4$ (a)0.2(b)0.6.

TABLE 1. XRD calculation.

Composition	Average Grain Size (nm)	Lattice Constant (Å)
$Mg_{0.2}Ni_{0.6}Co_{0.2}fe_2O_4$	23	8.211
$Mg_{0.4}Ni_{0.4}Co_{0.2}fe_2O_4$	22	7.960
$Mg_{0.6}Ni_{0.2}Co_{0.2}fe_2O_4$	21	7.210

TABLE 2. VSM calculation

Composition	Magnetization (emu/g)	Coercivity (G)	Retentivity (emu/g)
$Mg_{0.2}Ni_{0.6}Co_{0.2}fe_2O_4$	39.585	728.71	19.419
$Mg_{0.6}Ni_{0.2}Co_{0.2}fe_2O_4$	32.823	643.93	15.041

4. Conclusion

In the present study $Mg_xNi_{0.6-x}Co_{0.2}Fe_2O_4$ (where x = 0.2, 0.4, 0.6) have been synthesized using low temperature Sol-Gel Auto-Combustion method. From above xrd result we found that there is no significant change in particle size but change in Lattice constant of the material decreases as percentage of magnesium increases . As the percentage of magnesium increases the magnetization, Coercivity and retentivity decreases. The morphology seen from the SEM images for $Mg_xNi_{0.6-x}Co_{0.2}Fe_2O_4$ where x = 0.2, 0.4, 0.6 revealed that the MgNiCo ferrite does not have any specific morphology. From UV spectroscopy we found that band gap energy of the material is 2.72eV, it means sample is in nature of semiconductor.TEM micrograph shows material is crystalline in nature.

5. Acknowledgments

We thanks to our Department of Chemistry,We also thank the Department of C-MET Pune, IIT Powai and the Department of Physics, University of Pune for their kind co-operation and providing

their instruments for the purpose of characterization.

6. References

1. M. A. Gabal, Y. M. Al Angari and M. W. Kadi, *Polyhedron*, 30 (2011) 1185-1190.
2. A. T. Raghavender and K. M. Jadhav, Bull Mater. Sci., Vol. 32, No. 6, *Indian Academy of Sciences* December 2009, 575-578. 3. S. Zahi, *J. Electromagnetic Analysis and Applications, 2010, 2:56-62.*
3. S. Zahi, *J. Electromagnetic Analysis and Applications, 2010, 2:56-62.*
4. Dyal A, Loos K, Noto M et al (2003) *J Am Chem Soc* 125:1684
5. Tiefenauer LX, Tschirky A, Kuhne G et al (1996) *Magn Reson Imaging* 14:391
6. Skmoski R (2003) *J Phys Condens Matter* 15:R841
7. Gibbs MRJ, Opin C (2003) *Solid State Mater Sci* 7:83
8. Zhenxing Yue, Ji Zhou, Longtu Li, Hongguo Zhang, Zhiluin Gui, J*ournal of Magnetism and Magnetic Materials* 208 (2000) 55-60.
9. F.Li, H.Wang, L.Wang, J.Wang, J.Magn.Magn.Mater. 309 (2007) 295-299.
10. S.Sun, H.Zeng, D. B. Robinson, s. Raoux, P.M.Rice, S.X. Wang, G.Li, *J.Am.Chem.Soc. 126 (2004) 2782.*
11. T.Hyeon, Y.Chung, J.Park, S.S.Lee, Y.W. Kim, B.H.Park, *J.Phys.Chem. B 106 (2002) 6831*.
12. Q.Chen, Z.J. Zhang, J.Appl. Phys. 73 (1998) 3156-3158.
13. Skoog, et al. Principles of Instrumental Analysis. 6th ed. Thomson Brooks/Cole. 2007, 169-173.
14. *Suryawanshi SS,Deshpande V, Sawant SR:XRD analysis and magnetic properties of* Al^{3+} *substituted CuCd ferrite. J Mater Chem Phy 1999, 59:199-203*.
15. Suryawanshi SS, Deshpand V,Sawant SR: XRD analysis and magnetic properties of Al^{3+} substituted Cu-Cd ferrites. *J Mater Chem Phy 1999,59:199-203.*
16. E. C. Snelling (Ed), *Soft Ferrites, Properties and applications (*2nd Ed, Butter worth and Co. Ltd, London, 1988).118
17. R.S.Patil, S.V. kakatjar, S.A. Patil, A.M. Sankpla, S.R.Sawant, *Mater. Chem. Phys. 28 (1991) 355-365.*
18. [33] S.S. Bellad, S.C. Watawe, A.M.Sahikh, B.K. Chougule, *Bull.Mater.Sci. 23 (2) (2000) 83-85*.
19. [34] R. L. Coble, J. E Burke (Ed.), " sintering in ceramics", *Progress in ceramic Science, vol. 3, 197*
20. Skoog, et al. Principles of Instrumental Analysis. 6th ed. (Thomson Brooks/Cole. 2007), 169-173
21. Gajendra K. Pradhan, K. M. Parida, ACS Appl. Mater. Interfaces, 2011, 3 (2), 317-323.